DTA STUDY OF THERMAL DEGRADATION OF BAGASSE AND RICE STRAW HEMICELLULOSES

N. Shukry*, F. Ishak and Z. Sefain*

*DEPARTMENT OF CELLULOSE AND PAPER, NATIONAL RESEARCH CENTRE, DOKKI, CAIRO AND CHEMICAL DEPARTMENT, RAMSES STREET, CAIRO, EGYPT

DTA curves of the title substances were recorded up to 773 K, in static air. Bagasse hemicellulose (B) exhibited three overlapping exothermic effects, at 545, 618 and 700 K, while rice straw hemicellulose (R) displayed two exothermic effects, at 548 and 635 K. The absence of the third effect for R is ascribed to the catalytic effect of silica ash in promoting volatilization of the degradation products without allowing a "char residue" intermediate. The activation energy associated with each stage was derived by applying the Borchardt-Daniels general method, the Prout-Tompkins law, and integrated peak areas plotted as log $g(\alpha)$ vs. $1/T$. A second-order linearization of the data proved best, with apparent activation energies of 143, 249 and 289 kJ mol^{-1} for B, and 131 and 189 kJ mol^{-1} for R. The total peak areas for R, when normalized to ash-free mass, were equal to those evaluated for B, indicating that approximately identical energies are evolved in the temperature range studied.

Thermoanalytical studies on the pyrolysis or combustion of cellulosic materials have been subject of a large number of publications [1–18]. Three ranges of degradation are generally agreed upon: an early dehydration stage ($T < 423$ K), followed by fragmentation through random scission of the macromolecular structure, accompanied by the release of volatile components (423–523 K), and finally degradation of the carbohydrate residue, the evolution of gaseous products, their combustion and/or the glowing ignition of a "char residue" [7, 10, 14, 15, 18].

The second and third pyrolysis stages exhibit exothermic effects in DTA measurements, since they are associated with primary and/or secondary thermooxidation, active degradation, combustion and glowing ignition reactions.

In the evaluation of cellulosic materials with respect to their inflammability, three parameters were suggested by Košik *et al.* (15): (i) the maximum weight-loss rate (DTG), (ii) the percentage of the residue at the final

temperature (773 K) and (iii) the exothermic peak areas (DTA). This points to the use of thermoanalytical techniques (TG and DTA) to provide indications of the net endo- and exothermic procceses, or volatilization of the fuel caused by steadily rising temperatures.

In comparison with other wood components, it has been reported that hemicellulose is less thermally stable than cellulose and lignin, and that its active degradation begins at a lower temperature [3, 4, 6, 8, 9]. Nevertheless, little work has been published, particularly on the degradation stages and mechanisms for hemicellulose [1, 3, 9]. This initiated the present investigation, in which two hemicelluloses isolated from different parent materials were subjected to DTA. The resolved DTA peaks obtained were analyzed mathematically in order to derive the rate-controlling mechanism and also the activation energy associated with each pyrolysis stage.

Experimental

Materials

Bagasse (B) and rice straw (R) hemicelluloses were obtained from the depithed stalks and ground straw, immersed first in ethanolbenzene (1:1) for 6 h, and then air-dried. The dried paste was thereafter treated with an acetic acid - sodium chlorite mixture, and subsequently extracted by stirring in contact with 10% sodium hydroxide for 20 h at room temperature. The hemicellulose was next precipitated by the addition of 50% acetic acid (pH = 4–5), separated by decantation, solvent-exchanged with 75% ethanol, followed by 95% ethanol and ether, and finally dried under vacuum over calcium chloride.

The relative sugar contents of the products were estimated by current methods [19–21], which indicated the following contents. For hemicellulose B, the values were: xylose = 58.5%, arabinose = 25.7%, glucose = 12.0% and galactose = 3.5%.

Hemicellulose R gave values of: xylose = 54.8%, arabinose = 18.0%, glucose = 21.0% and galactose = 6.2%. Hemicellulose B proved to be ash-free, whereas hemicellulose R was contaminated by the presence of 26% ash (mainly silica).

Procedures for DTA peak analysis

Mathematical analysis was performed according to the following correlation procedures:

A. The method of Borchardt and Daniels (BD) [22]

Their equation describing the first-order decomposition followed along the DTA peak has the form

$$k = \frac{\Delta T}{(A - a)} \qquad (n = 1) \tag{1}$$

where k is the reaction rate constant, A is the total area of the DTA peak, a is the area covered up to temperature T, ΔT is the amplitude of the DTA peak at temperature T and n is the order of the conversion. A linear relationship should appear for the plot $\ln k$ *vs.* $1/T$, according to the Arrhenius expressions

$$k = A \exp(-E/RT) \tag{2}$$

and

$$\ln k = \ln A - E/RT \tag{3}$$

The values of E and $\ln A$ are readily evaluated from the slope and intercept of Eq. (3).

Another linearizing method has been derived by Piloyan *et al.* [23], their final equation being

$$\ln \frac{\Delta T}{(1 - \alpha)^n} = C - E/RT \tag{4}$$

This equation is in fact a generalized form of Eq. (1), where $(1 - \alpha)$ stands for $(A - a)$, for $\ln A$, and $n = 1$ (note that $\frac{A - a}{A} = (1 - \alpha)$, with $\alpha = \frac{a}{A}$.

In the present investigation, plots were made for Eq. (4) by correlating the left-hand side with $1/T$, for $n = 1$, 1.5 and 2. An example of the linear plots is presented in Fig. 1, for peak 1 for hemicellulose B.
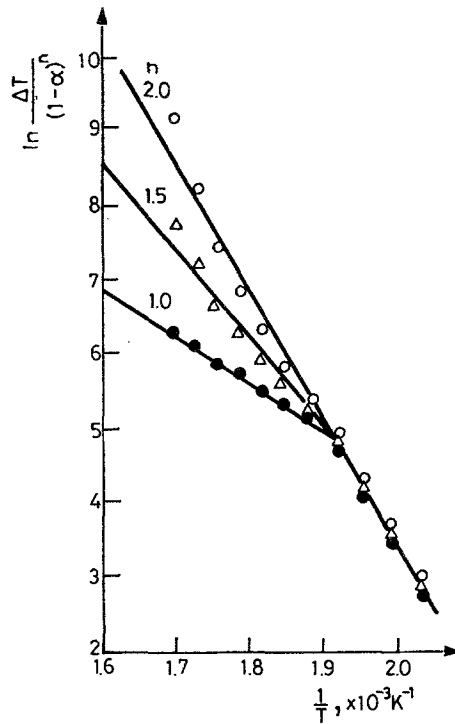
Fig. 1 Application of the Borchardt-Daniels general equation on the 1st DTA peak of hemicellulose (B)

B. The equation of Prout and Tompkins (PT)

An old decomposition law, designated as a nucleation growth-controlled [24], branching nuclei [25] or autocatalytic reaction (Prout-Tompkins law) [26], was found applicable in the present analysis. It has the form

$$k = \ln\frac{\alpha}{1-\alpha} \qquad (5)$$

where α has the same meaning as before, i.e. $\alpha = \dfrac{a}{A}$. Thus, a plot of $\ln\dfrac{\alpha}{1-\alpha}$ vs. $1/T$ was tried, and a modified form of the same law was tested by using $\ln\dfrac{\alpha}{(1-\alpha)^2}$. An illustrative plot is shown in Fig. 2. Nevertheless, linear regression analysis was employed, associated with the method of least squares, instead of graphical plotting throughout.
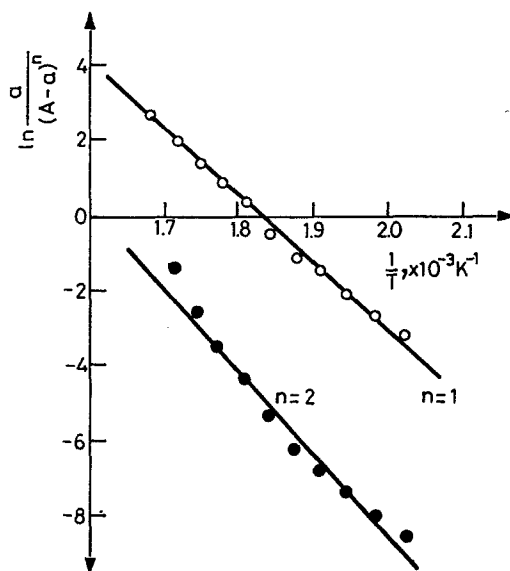
Fig. 2 Application of the Prout-Tompkins law on the 1st DTA peak of hemicellulose (B)

C. Integrated peak area and amplitudes, treated as TG waves

This was recently proposed by Girgis and Petro [27]. The mathematically integrated peak areas, or the summed peak amplitudes measured in regular temperature intervals (10 deg), are plotted as $\alpha = f(T)$ curves ($\alpha = \dfrac{a}{\Sigma a}$ or $\dfrac{h}{\Sigma h}$) where a and h denote the specific strip area or peak amplitude at temperature T along the whole DTA peak. Analysis of such integral curves was performed by correlating $g(\alpha)$ vs. $1/T$ as suggested by Satava and Skvara [28]. Testing was performed only for the second-order mechanism expression (SO) since this mechanism proved to be the most suitable for the TG curves of the same materials [29].

The correlation of $g(\alpha)$ with $1/T$ was tested by applying, likewise, linear regression analysis with the least squares method.

Differential thermal analysis of the hemicelluloses

The thermal characteristics were recorded with an apparatus produced by Netzsch-Gerätebau GmbH, Germany. A linear heating rate of 5 deg/min was adopted, in the presence of static air, up to 873 K.

Results and discussion

Differential thermal characteristics

Figure 3 illustrates DTA tracings for hemicelluloses R and B indicating a single broad endothermic effect at low temperatures, followed by prominent overlapping exothermic reactions. Hemicellulose B exhibits a series of three such exotherms, but hemicellulose R only two exothermic effects. These thermal effects were separated to obtain the peaks shown as dotted lines in the same Figure. It should be noted that the overlapping third (and fourth) thermal effects shown by hemicellulose B were not resolved, but were regarded as one effect, due to the small temperature range covered by such reactions.
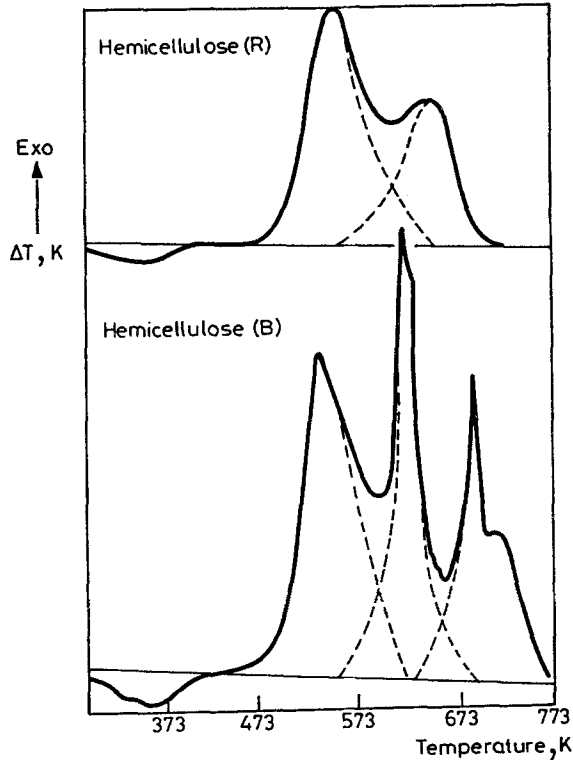

Fig. 3 DTA curves of hemicelluloses (R) and (B)

Although the present recordings were not made in a DSC cell, they were carried out under the same conditions: rate of heating, DTA sensitivity, amplification, recording speed and atmosphere of static air. Thus, it may be safe to consider the integrated peak area (Σa or A_p) or amplitude (Σh_p) as semiquantitative measures of the comparative heat evolved in the exothermic stages [32, 33]. These were normalized with respect to the sample mass, and also to the ash-free (AF) mass, as shown in Table 1.

Table 1 Description of the thermal effects of degradation stages

a - Hemicellulose (R)

Stage	DTA peak						TG wave		
	T_p, K	A_p	h_p	Σh_i	A_p(AF)	Σh_i (AF)	$T_{0.5}$	%loss (AF)	T_{max}, K
1st	548	206	92	693	362	1217	517	57.3	523
2nd	648	114	57	392	200	688	616	27.9	630

b - Hemicellulose (B)

Stage	DTA peak				TG wave		
	T_p, K	A_p	h_p	Σh_i	$T_{0.5}$	%loss	T_{max}, K
1st	538	242	122	813	518	59.1	522
2nd	623	197	172	581	612	16.0	625
3rd	685 709	132	74 56	390	684	7.0	691

(T_p) Temperature peak maximum,

(h_p) Maximum peak height in arbitrary units,

(Σh_i) summation of peak magnitude,

(A_p) total peak area,

(AF) normalized to ash free substance,

($T_{0.5}$) Temperature at 50% conversion,

(T_{max}) temperature $\alpha = 0.632$

A first look at the directly measured integrated peak areas or amplitudes (estimated in arbitrary units, AU) indicates that hemicellulose B liberates more energy on degradation. This is clear for each of its first two exothermic effects, whether taken as Σa or Σh_p. Columns 5 and 6 (Table 1/a) give the normalized cummulative areas or amplitudes expressed for the same or the

AF mass. It appears that the heat (expressed as Σa or Σh_p) evolved by hemicellulose R) surpasses that for hemicellulose B in the first two stages. However, it is of interest to observe that the total heats evolved (the sum of the three A_p values for hemicellulose B and that of the two A_p values for hemicellulose R are identical.

This led us to conclude that, although the two hemicelluloses exhibit apparently different DTA thermal effects (two as compared to three or more peaks), the total heats evolved in the exothermic stages are the same. It should be recalled that the cumulative peak areas express the heat evolved more exactly, since the cumulative peak amplitudes depend on the distances between the successively measured ΔT values. However, if these were made infinitesimally small, their summation would yield the same peak area. This could explain the apparently small discrepancies between the Σa and Σh values for the two substances

A DTA peak in this case could be regarded as a good approximative estimate for the comparison of different cellulosic materials measured under identical conditions. Accordingly, the inorganic residue is considered to act as a diluent in comparison with the ash-free cellulosic substance. In other words, independently of the inorganic residue, the same total heat is evolved upon combustion of the two different hemicelluloses; this is true whether the combustion takes place in two or more stages.

Comparison of TG and DTA degradation stages

In the TG curves, hemicellulose B displays three and hemicellulose R two weight-loss peaks [29]. However, it may be seen (Table 1) that:

(a) The TG effects do not overlap and are easily separated into the consecutive stages.

(b) The temperature of maximum weight loss at 50% conversion ($T_{0.5}$) is in each case lower than the corresponding peak temperature (T_p). Although the maximum reaction rate (T_{max}) has been suggested to be located at a fractional conversion of 0.632 [31], the values of T_{max} for hemicellulose R are still lower than T_p.

(c) It seems that there is no correlation between the weight lost in each degradation stage and the corresponding DTA peak area (A_p) or maximum peak amplitude (h_p). Thus, for hemicellulose B in the first exothermic stage, for example, a considerable weight loss ($\sim$60%) is accompanied by an apparent heat of 240 AU (DTA peak area), whereas a small weight loss of 7% is displayed in more than half the DTA peak area. This could indicate that different heats are evolved in the different stages. The first one is probably

the algebraic sum of the heat absorbed in the degradation and that evolved in the combustion of the volatile products. Otherwise, the combustion of the late-stage products (supposed to be char) evolves more heat than the combustion of the primary gaseous products.

This would lead us to conclude that exactly similar thermal effects are not observed in the simultaneously recorded TG and DTA curves, especially for such naturally polymeric substances as hemicelluloses. Further, the net thermal effects are not completely comparable. In the high-temperature range (say $T \geq 600$ K), the overlapping processes of depolymerization, thermooxidation, dehydration and combustion of the released gaseous products would be indicated by a net small weight-loss change. On the other hand, such simultaneous processes could show a high net exothermic effect due to the high combustion heat relative to the low heat needed for degradation of the macromolecular structure and/or fragmentation and dehydration. Nevertheless, the simultaneously obtained TG and DTG curves are not to be discriminated, as they are in fact complementary to each other in an elucidation of the ongoing degradation processes. As previously pointed out by Shafizadeh [5], TG and DTA provide an indication of the net balance between endo- and exothermic reactions, or volatilization of the cellulosic substance caused by steadily rising temperature.

Derivation of the kinetic parameters of degradation

As pointed out above, various procedures were employed: the method of Borchardt and Daniels (BD), the equation of Prout and Tompkins (PT) and the integrated peak areas or amplitudes. The first two methods were tried with $n = 1$-2, whereas in the third method only a second-order expression was tried. Table 2 lists the activation energies obtained, and also the ranges of applicability of the linear correlation coefficients.

Application of the BD method, allowing for a change in n results in a better linearization with increase in n, accompanied by an increase in the activation energy. The high-order expression gives the best linearization for most of the five analyzed peaks. The PT law applies equally well, particularly with $n = 1$, and exhibits highly satisfactory correlation coefficients. The two suggested procedures for peak area integration, or amplitude summation, can be applied equally satisfactorily to the present data. It should be recalled that, if the distance between the successive peak amplitudes is made sufficiently small, their sum would yield the cumulative peak area.

A classical method used for the determination of reaction order from the peak shape was also tried: that of Kissinger [30]. For the three exothermic

Table 2 Estimated activation energies of degradation E_a kJ $\cdot$ mol^{-1}

Method of peak analysis		Hemicellulose (R)		Hemicellulose (B)		
		1st peak	2nd peak	1st peak	2nd peak	3nd peak
Borchardt & Daniels						
$\ln \dfrac{\Delta T}{(1-\alpha)}$	Range*	0.38–0.91	0.05–0.91	0.25–0.94	0.05–0.50	0.05–0.85
	E_a	48	123	55	210	75
$\ln \dfrac{\Delta T}{(1-\alpha)^{1.5}}$	Range*	0.26–0.91	0.05–0.70	0.18–0.88	0.05–0.75	0.05–0.85
	E_a	89	149	99	210	150
$\ln \dfrac{\Delta T}{(1-\alpha)^{2}}$	Range*	0.16–0.91	0.05–0.70	0.04–0.88	0.05–0.95	0.05–0.85
	E_a	128	176	143	224	221
Prout-Tompkins						
$\ln \dfrac{a}{A-a}$	E_a	132	200	142	237	296
	$-r$**	0.998025	0.986792	0.997817	0.994875	0.968624
$\ln \dfrac{a}{(A-a)^{2}}$	E_a	191	295	206	345	468
	$-r$**	0.989454	0.969842	0.980172	0.984544	0.993454
Summation method						
Σa	E_a	128	194	144	247	305
	$-r$**	0.997481	0.989157	0.994463	0.986638	0.996534
Σh	E_a	135	185	143	288	302
	$-r$**	0.997265	0.988050	0.999067	0.993594	0.993039

* Range of applicability of the specific equation

** The linear correlation coefficient

peaks of hemicellulose B the estimated reaction orders were 1.93, 2.12 and 1.97, whereas for hemicellulose R the corresponding values for the two DTA peaks were 1.62 and 1.12. Accordingly, selection was made for the second-order results evaluated from the BD method and the integrated DTA peak, as well.

On the basis of the postulates put forward previously for the analysis of TG waves, the first degradation stage for both hemicelluloses involves the same processes, irrespective of the parent source. Such a stage is a very prominent one, as it is associated with the loss of ~60% for either material. This is generally related with the initial degradation reactions of depolymerization, hydrolysis, oxidation, dehydration and decarboxylation [5].

The second stage, displayed as a single DTA peak (or TG wave) for hemicellulose R, appears as a series of two or more peaks for hemicellulose B. Degradation of the latter substance was suggested to proceed through the combustion of volatile degraded components and the formation of a "char residue" that is oxidized in a subsequent stage. The structural silica present in hemicellulose R was likewise suggested to catalyze the direct combustion of the degradation products without the formation of an (intermediate) char. Thermal decomposition on the surface of the active ash (>60% at 523 K), and adsorption of the volatile products, lead to their cracking and combustion with a lower activation energy. The ash probably acts here as a diluent for the reacting material (cf. the peak areas in this range, and also the maximum peak amplitude). Reference here is made to the estimated reaction order for this stage for hemicellulose R, which drops to a first-order reaction in this catalyzed state. This could possibly account for the apparently low exothermic energy for this stage in comparison with that for hemicellulose B. Glowing combustion may be the essential third stage exhibited for the purely organic, ash-free hemicellulose B [15].

References

1 B. Salomon, G. Rozmarin, A. Biro and Cr. Simionescu, Cellul. Chem. Technol., 1 (1967) 601.
2 F. Abe, Mokuzai Gakkaishi, 14 (1968) 98.
3 M. Kosik, L. Geratova, F. Rendos and R. Domansky, Holzforsch. Holzverwert., 20 (1968) 15.
4 O. Swabe, T. Sadoh, K. Kitas and A. Sato, Mokuzai Gakkaishi, 14 (1968) 104.
5 F. Shafizadeh, Advances in Carbohydrate Chemistry, M. L. Wolfrom and R. S. Tipson, Eds., Vol. 23, 1968 p. 418.
6 M. V. Ramiah and D. I. Goring, Cellul. Chem. Technol., 1 (1969) 277.
7 M. V. Ramiah, J. Appl. Polym. Sci., 14 (1970) 1323.
8 K. Nemeth and I. Szendrey, Erdészeti Faipari Egy. Tud. Közl., (1973) 117.
9 T. Hirata and H. Abe, Mokuzai Gakkaishi, 19 (1973) 451.
10 F. Shafizadeh and A. G. W. Bradbury, J. Appl. Polym. Sci., 23 (1979) 1431.
11 A. G. W. Bradbury, Y. Sakai and F. Shafizadeh, J. Appl. Polym. Sci., 23 (1979) 3271.
12 F. Shafizadeh, R. H. Furneaux, T. G. Cochran, J. P. Scholl and Y. Sakai, J. Appl. Polym. Sci., 23 (1979) 3523.
13 E. Chronet and C. Roy, Thermochim. Acta, 35 (1980) 389.
14 D. Dollimore and J. M. Hoath, Thermochim. Acta, 45 (1981) 87.

15 M. Košik, V. Reiser and A. Blazej, J. Thermal Anal., 23 (1982) 51.
16 W. S. I. Mok and M. J. Antal, Jr., Thermochim. Acta, 68 (1983) 155.
17 G. Chauvette, M. Heitz, M. Rubio, J. Khorami, E. Chronet and H. Menard, Thermochim. Acta, 84 (1985) 1.
18 P. Roque-Diaz, V. Zh. Shemet, V. A. Lavrenko and V. A. Khristich, Thermochim. Acta, 93 (1985) 349.
19 G. Jayme and P. Sarten, Naturwiss., 28 (1940) 822; Biochem. Z., 308 (1941) 109.
20 R. L. Whistler and D. E. B. Gaillard, Arch. Biochem. Biophys., 93 (1961) 332.
21 R. L. Whistler, Methods of Carbohydrate Chemistry, Vol. 1, 1962 p. 388.
22 H. J. Borchardt and F. Daniels, J. Phys. Chem., 79 (1957) 41.
23 G. O. Piloyan and O. S. Novikova, Russ. J. Inorg. Chem., 12 (1967) 313.
24 J. Ribas, M. Serra and A. Escuer, Thermochim. Acta, 91 (1985) 107.
25 H. Tanaka, S. Shimada and H. Negita, Int. J. Chem. Kin., 17 (1985) 149.
26 H. Tanaka and M. Tokumitsu, J. Thermal Anal., 29 (1984) 87.
27 B. S. Girgis and N. Sh. Petro, J. Thermal Anal., 34 (1988) 363.
28 V. Satava and F. Skvara, J. Amer. Chem. Ceram. Soc., 52 (1969) 591.
29 N. Shukry, B. S. Girgis and M. Z. Sefain, Bull. Soc. Chim. Fr., accepted for publication
30 H. E. Kissinger, Anal. Chem., 29 (1957) 1702.
31 H. H. Horowitz and G. Metzger, Anal. Chem., 35, 10 (1963) 1465.
32 R. L. Bohon, Proc. 1st Toronto Symp. Therm. Anal., Ed. H. G. McAdie, Toronto 1965, p. 63.
33 T. R. Ingraham and P. Marier, Can. Met. Quart., 4 (1965) 169.

Zusammenfassung — In statischer Luftatmosphäre wurden die DTA-Kurven der Titelsubstanzen bis 773 K aufgenommen. Bagasse-Hemizellulose (B) zeigte bei 545, 618 und 800 K drei überlappende exotherme Effekte, während sich bei Reisstroh-Hemizellulose (R) zwei exotherme Effekte bei 548 und 635 K ergaben. Das Fehlen des dritten Effektes für R wird dem katalytischen Effekt von Kieselerdeasche bei der Förderung des Freisetzen der Abbauprodukte zugeschrieben, ohne "koksige" Zwischenprodukte zuzulassen. Die zu den einzelnen Stufen gehörenden Aktivierungsenergien wurden durch Anwendung der allgemeinen Borchardt-Daniels-Methode, des Prout-Tompkinsschen Gesetzes und der graphischen Darstellung der integrierten Peakflächen in einem $\log g(\alpha)$ vs.$1/T$ Diagramm erhalten. Eine quadratische Linearisierung der Daten ergab die besten Ergebnisse mit den scheinbaren Aktivierungsenergien von 143, 249 und 289 kJmol^{-1} für B und mit 131 und 189 kJmol^{-1} für R. Die totalen Peakflächen für R zeigen nach Normalisierung auf aschefreie Massen die gleichen Werte, die auch für B erhalten wurden.